Semiconductor Physics, Quantum Electronics & Optoelectronics, 2026. V. 29, No 3. P. 292-301.

Semiconductor physics

Femtosecond laser processing of titanium dioxide films prepared with sol-gel method

I.M. Dmytruk[1], N.I. Berezovska[1], P.A. Manoryk[2], N.I. Romanovska[2], G.P. Podust[1], Ye.S. Hrabovskyi[1], P.S. Khort[1], O.S. Kondratenko[3], V.R. Romanyuk[3], S.V. Mamykin[3]

[1]*Taras Shevchenko National University of Kyiv, 64/13, Volodymyrska street, 01601 Kyiv, Ukraine*
[2]*L.V. Pisarzhevsky Institute of Physical Chemistry, National Academy of Sciences of Ukraine, 31, prospect Nauky, 03028 Kyiv, Ukraine*
[3]*V. Lashkaryov Institute of Semiconductor Physics, National Academy of Sciences of Ukraine, 41, prospect Nauky, 03680 Kyiv, Ukraine*
[*]*Correspondence author e-mail: nataliya.berezovska@knu.ua*

Abstract. The self-cleaning and photocatalytic properties of TiO_2 films are crucial for coating of optical elements that operate in harsh environmental conditions. During our research, the optimal chemical composition of the sol-gel mixture and conditions for spin-coating of TiO_2 films were selected. Ellipsometry studies showed that before calcination at 450 °C, the TiO_2 film on glass had a thickness of 247 nm and was quite porous with significant roughness. After calcination, the thickness of the TiO_2 film decreased to 89 nm. It became significantly denser. Further modification of TiO_2 films was performed using femtosecond laser pulses with a wavelength of 800 nm. Treatment of TiO_2 films with laser radiation resulted in the formation of laser-induced surface features, including nanoparticles and nano-cracks. The selected laser processing conditions were aimed to maintain sufficient transparency of the TiO_2 film that was achieved at the density of irradiation pulse energy of 0.025 J/cm^2. The laser-treated surface exhibits improved hydrophilic properties. The optical properties of TiO_2 films on glass, studied using photoluminescence and Raman scattering, showed that after post-synthetic processing, including femtosecond laser treatment, a predominantly anatase crystal structure was formed.

Keywords: titanium dioxide, thin film, sol-gel method, femtosecond laser pulses, laser-induced surface structures, photoluminescence, Raman scattering.

https://doi.org/10.15407/spqeo29.03.292
PACS 78.30.Fs, 78.55.-m, 79.20.Ds, 81.20.Fw

Manuscript received 31.10.25; revised version received 10.12.25; accepted for publication 16.09.26; published online 25.09.26.

1. Introduction

Titanium dioxide (TiO_2) coatings on various substrates are actively used for photocatalysis, self-cleaning coatings, improvement of corrosion resistance, electron transport layer in thin solar cells, *etc*. [1, 2]. Under the influence of UV radiation, TiO_2 becomes superhydrophilic and begins to attract moisture from the air, which can collect dirt from the surface, due to electrochemical reactions including oxidative decomposition of pollutants [3, 4]. TiO_2 is of particular interest due to its multiple polytypes (brookite, anatase, and rutile), which form under different conditions and can transform into each other. All TiO_2 polytypes have large refractive indices ($\sim 1.93 < n < 2.6$ at $\lambda = 633$ nm) and high transparency within the visible spectral range. TiO_2 is a wide-bandgap semiconductor ($E_g > 3$ eV). Rutile and anatase polytypes of TiO_2 are technologically promising crystal structures for the aforementioned applications. The anatase polytype has a higher optical band gap than the rutile (~ 3.2 *vs* 3.0 eV) [5]. The properties of TiO_2, including light absorption and charge transfer, are closely dependent on its defect composition, which is important for the utilization of solar energy, the photocatalytic properties, *etc*. Oxygen vacancies, interstitial titanium atoms, and titanium vacancies are considered as defect states in TiO_2 [6]. The equilibrium concentration of these defects and their slow transfer from the surface to the bulk were determined.

The main chemical methods for producing titanium dioxide-based films include chemical vacuum deposition, chemical evaporation, the sol-gel method, and fusion.

Among the proposed approaches, the sol-gel method is the most attractive, as it allows for regulating the physicochemical characteristics of the films by varying the qualitative and quantitative chemical composition of the film-forming composition, the conditions of sol formation, and the conditions of post-synthetic processing.

An improvement of photocatalytic activity can be achieved by increasing the light absorption capacity of the material based on TiO_2, and requires an expansion of the light absorption range of TiO_2 into the visible region. Creating localized energy levels in the band gap could promote the excitation of electrons from the valence band to levels induced by the dopant that could improve light absorption of TiO_2 [7]. Regarding the photocatalytic efficiency of different TiO_2 polytypes, anatase prevails over the more stable rutile. This can be explained by the higher density of localized states, and, as a result, surface-adsorbed hydroxyl radicals, as well as the slower recombination of charge carriers in anatase compared to rutile, which contributes to the improvement of photocatalytic capacity. It was stated that the anatase-rutile mixture exhibits better photocatalytic properties due to improved separation of charge carriers.

The ultrashort laser pulses provide a simple, fast, and reliable method for contactless modification of thin films due to a minimal thermal effect and high precision in both lateral and vertical processing [8]. The number of publications devoted to femtosecond laser structuring of TiO_2 films is insignificant, but has begun to increase in recent years, demonstrating the prospects of this method for obtaining TiO_2 surfaces with properties that are interesting for practical applications [9–12].

Laser treatment of sol-gel-derived TiO_2 films offers broad opportunities to tailor film characteristics, namely thickness, crystalline or amorphous structure, grain size, residual stress, and defect density [13]. Compared to other surface treatment methods, laser processing uniquely combines time, temperature, and other conditions that are otherwise unattainable, and it offers high selectivity. Unlike thermal processing, laser irradiation is extremely fast and affects only the thin surface film. The influence of laser treatment of TiO_2 films on their resulting wettability and photocatalytic activity is of particular interest. Since the influence of laser-induced surface structuring on the wettability of metals and semiconductors is widely known, it is reasonable to expect an influence of laser treatment on these characteristics of TiO_2.

Now we present the development of functional TiO_2 films on glass substrates and their subsequent processing with femtosecond laser radiation.

2. Experimental details

Titanium dioxide thin films have been prepared by the sol-gel spin-coating method on a glass substrate [14]. Titanium tetra-isopropoxide as a starting material was dissolved in i-propanol, then a calculated amount of block-copolymer Pluronic P-123 and nitric acid was added. The obtained sol was stirred for 2 hours. The resulting sols were deposited on the glass substrates 1×2 cm by spin-coating at 500 rpm for 1 minute. The resulting films were dried in an oven at 100 °C for 4 hours, then transferred to a muffle furnace and calcined at 450 °C for 2 hours at a heating rate of 2 °C/min.

The laser modification of TiO_2 films has been performed with a Ti:sapphire femtosecond laser system based on a Mira-900F femtosecond oscillator with a Legend-HE chirped pulse amplifier (Coherent, USA) using ultrashort laser pulses with a fundamental wavelength of 800 nm, a pulse duration of 150 fs, and a pulse repetition rate of 1 kHz. A laser beam with an average power close to 450 mW was focused on the sample by a spherical lens with a focal length of 100 mm. The samples were placed in front of and behind the focus to prevent the effect of air ionization in the focus on the processing. To vary the power density of the laser radiation on the surface, the sample surface was placed at different distances from the focus (usually from 5 to 20 mm). An average laser power was controlled by a laser power meter “Field Master GS” with a detector head “LM-10” (Coherent, USA). The horizontally polarized laser beam was incident normally onto the sample surface. The sample was placed on the 3-axis motorized stage, which provided sample scanning at different speeds (typically at 0.5–1 mm/s) perpendicular to the beam. The laser processing has been performed in air in the multi-pulse regime, creating an area sufficient for spectroscopic studies and wettability estimation. The distance between individual passes was 0.2 mm, which ensured partial overlap of the neighbor passes.

The morphology of the obtained TiO_2 films after ultrafast laser processing has been analyzed using a scanning electron microscope (SEM) AURA 100 (SERON Technology Inc., Republic of Korea). The ellipsometric parameters were measured using a Semilab SE-2000 spectral ellipsometer (Semilab Semiconductor Physics Laboratory Co. Ltd., Hungary). Transmission (absorption) spectra were measured using a Cary 60 spectrometer (Agilent Technologies, USA) at room temperature.

The photoluminescence (PL) spectra of the TiO_2 films were excited by the third harmonic (wavelength of 266 nm) of a Ti:sapphire femtosecond laser “Mira Optima 900-F” (“Coherent”, USA). Output power – 16 mW, pulse repetition frequency 76 MHz. The excitation beam was focused on the sample by using the 100 mm cylindrical lens in an area equal to 0.2×3 mm^2. Spectra were recorded using an Acton Research SP-2500i spectrometer with a cooled CCD detector. Measurements were performed at room temperature.

The Raman spectra of the TiO_2 films on Si substrate have been recorded in backscattering geometry using the RM1000 μ-Raman spectrometer (Renishaw, UK) with excitation at 532 nm at room temperature. The spectral resolution is 0.3 cm^{-1}. The main Si phonon peak at 520.5 cm^{-1} was used as a reference for the Raman measurements.

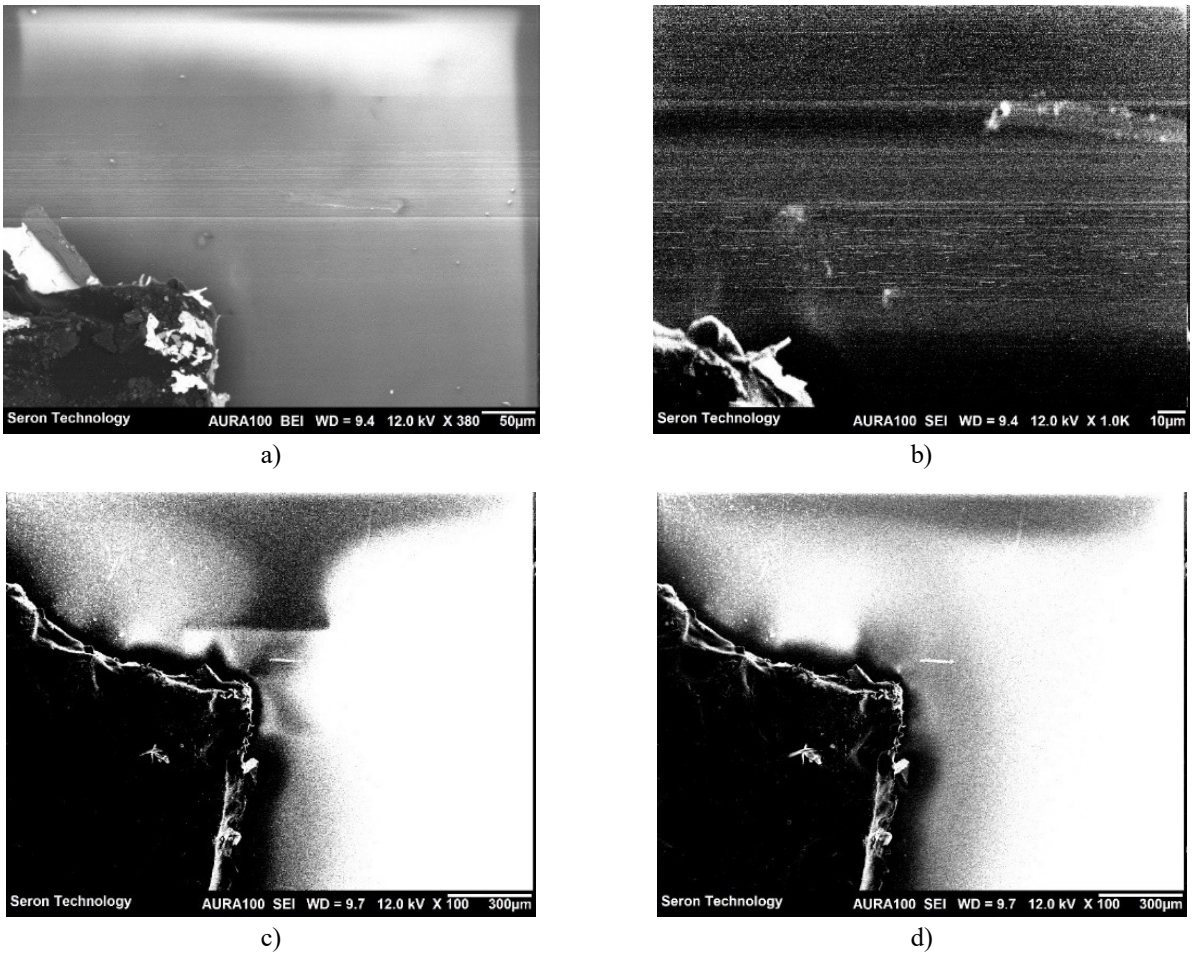

Fig. 1. Scanning electron microscopy of a TiO_2 film on glass. Image obtained with a mirror-reflected electron detector (a) and a secondary electron detector (b). Time-sequential images of the same area (c, d) show the gradual dissipation of surface charge.

3. Results and discussion

The transparent TiO_2 films were obtained by the sol-gel method and annealed at 450 °C. The presence of P-123 in the reaction mixture provides stability, homogeneity, and viscosity of the obtained TiO_2 sol as well as an ordered oxide structure.

Fig. 1 shows SEM images of the TiO_2 film surface on a glass substrate after deposition and annealing in an oven at 450 °C. The SEM image obtained using a specularly reflected electron detector (Fig. 1a) shows high film homogeneity within a scale of hundreds of micrometers. However, it shows the effects of charge accumulation on the film surface (white stripes in the upper right corner). To reduce these effects, SEM observations were carried out near the carbon electrode, which provided electrical contact to the surface. Its edge can be seen in the lower left corner. The white particles on the black carbon are gold microparticles, which were used to focus the microscope. The dynamics of the transformation of the shape of the stripes caused by the surface charge (Figs. 1c, 1d) show that the film still has nonzero conductivity. Indeed, when switching from a larger magnification to a smaller one, a light rectangle from the previous frame can be seen in the image, which disappears after a few seconds.

The investigation of the effect of thermal treatment on the thickness and optical constants of TiO_2 films was carried out using spectroscopic ellipsometry. The measurements of the ellipsometric parameters (Ψ and Δ) were performed at an angle of incidence of 60° within the spectral range 0.6…5.0 eV. To determine the optical constants (refractive index n and extinction coefficient k), as well as the film thickness d, the experimental data were analyzed, minimizing the root-mean-square error (RMSE) between the measured and model-generated pseudo-dielectric function spectra ($\langle\varepsilon_1\rangle$ and $\langle\varepsilon_2\rangle$) (Fig. 2).

The Tauc–Lorentz model [15] was used to describe the dispersion of the optical constants of the TiO_2 layer. This empirical model, developed specifically for amorphous dielectrics and semiconductors, correctly describes the shape of the absorption edge by limiting interband transitions with the optical band gap (E_g). We have previously successfully applied this methodological approach to the ellipsometric analysis of nanostructured oxide films, particularly ZnO [16–18]. The quantitative results of the ellipsometric modeling for the investigated samples are summarized in Tables 1 and 2.

Table 1. Optical model parameters of the TiO_2 films obtained from the analysis of spectroscopic ellipsometry data (Tauc–Lorentz dispersion model).

Film state	Model structure	Layer thickness d, nm	Roughness drough, nm	Refractive index n (at 633 nm)	E_g, eV	R^2
Dried (100 °C)	Glass / TiO_2 / EMA	250.9 ± 0.2	12.8 ± 0.3	1.601	3.51	0.987
Annealed (450 °C)	Glass / TiO_2	86.8 ± 0.1	< 0.5	1.872	3.63	0.997

Table 2. Best-fit parameters of the Tauc–Lorentz and Lorentz oscillators used to model the optical dispersion of the TiO_2 films.

Parameter	Dried film (100 °C)	Annealed film (450 °C)
Tauc–Lorentz oscillator		
A (eV)	297.09	185.81
E_0(eV)	1.71	4.11
C (eV)	2.44	1.97
E_g (eV)	3.51	3.63
High-frequency dielectric constant		
ε_∞	1.77	1.84
Lorentz oscillator*		
f	0.12	–
E_0 (eV)	7.11	–
Γ (eV)	1.53	–

*The Lorentz oscillator was additionally required for the dried sample to account for high-energy absorption tails originating from the unburned organic components.

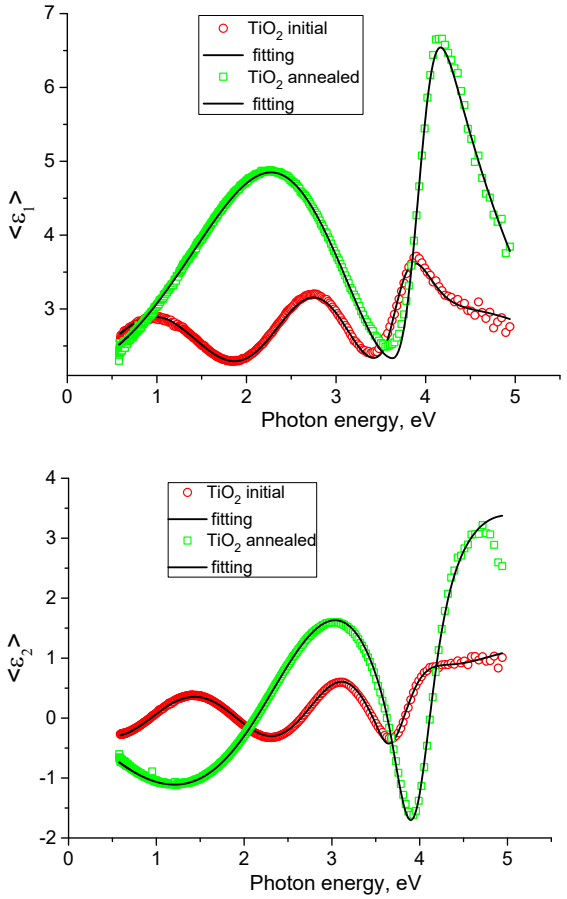

Fig. 2. Experimental (symbols) and model-calculated (solid lines) spectra of the real ($\langle\varepsilon_1\rangle$) and imaginary ($\langle\varepsilon_3\rangle$) parts of the pseudo-dielectric function for TiO_2 films on glass substrates: after drying at 100 °C (red curves) and after annealing at 450 °C (green curves).

For the film, after deposition and drying at 100 °C, the optical model included the substrate (glass), the main TiO_2 layer, and a thin surface roughness layer (~13 nm) described by the effective medium approximation (EMA). The total thickness of such a film was ~ 264 nm. The calculated refractive index at 633 nm is n ~ 1.60. This relatively low value indicates that the film at this stage is highly porous and amorphous. The nanocomposite contains a significant amount of residual organic components (Pluronic P-123 block copolymer) and solvent. The optical band gap (E_g) of this amorphous phase was estimated to be equal to 3.51 eV.

After thermal treatment at 450 °C for 2 hours, radical changes in the optical characteristics are observed, confirming the structural reorganization of the matrix. The best fit to the experimental data ($R^2 > 0.996$) was achieved for a single-layer model with surface roughness, indicating the formation of an optically homogeneous film.

One can see from Fig. 3 and Table 1 that the film thickness after annealing catastrophically decreased by a factor of three, down to ~ 87 nm. This strong densification is a direct consequence of the evaporation of solvent residues, complete burnout of the organic template, and the collapse of the inorganic framework. Simultaneously, the refractive index n (at 633 nm) significantly increased from 1.60 to 1.87. This increase indicates the crystallization of the material (predominantly into the anatase phase) and the formation of a denser inorganic network. The value n ~ 1.87 is characteristic of mesoporous crystalline TiO_2 films, where the presence of pores slightly reduces the effective refractive index compared to the bulk material (n ~ 2.4…2.5).

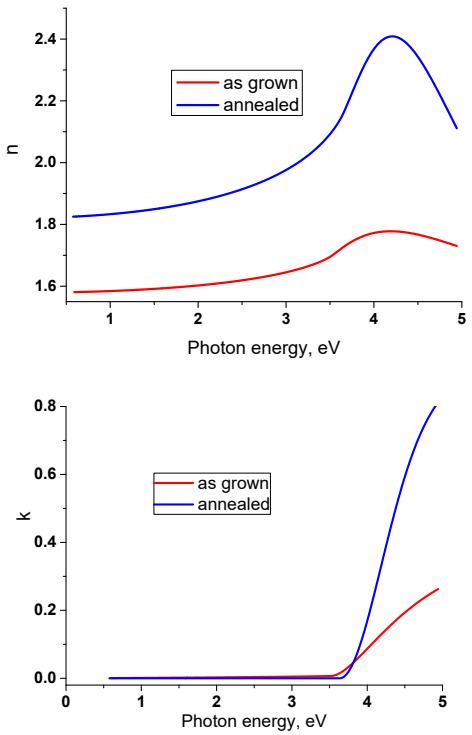

Fig. 3. Spectral dependences of the refractive index (n) and extinction coefficient (k) of TiO_2 films before (red lines) and after thermal treatment at 450 °C (blue lines), extracted from ellipsometric data using the Tauc–Lorentz model.

The annealed film demonstrates absolute optical transparency within the visible range (extinction coefficient $k \to 0$), confirming the absence of defect-induced absorption or carbon residues. The optical E_g, determined from the Tauc–Lorentz model, was ~ 3.63 eV, slightly higher than for the non-annealed film.

The treatment of TiO_2 films with femtosecond laser radiation resulted in the formation of laser-induced surface features, including nanoparticles, nanocracks, and other features.

In our experiments, only a few basic processing parameters are varied, which allows us to single out their influence on the resulting structures during further studies of the samples. It also minimizes the need to realign the laser system during a series of experiments, which reduces the probability of uncontrolled changes in irradiation parameters (*e.g.,* intensity distribution in the beam cross section), which can occur with complex optical schemes even with minor displacements of optical components.

A separate task was to select the power density of femtosecond radiation, which should be close to and slightly beyond the ablation threshold of the material (in this case, TiO_2 film), but not exceed it. We were guided by certain conclusions from studies on the ultrashort laser structuring of thin films, which are presented in [8, 19].

Irradiating the samples on a glass substrate, we obtained different areas with varied laser parameters (Figs. 4a, 4b). For the sample TiO_2 film on glass without calcination, area N1 was treated with radiation power of 450 mW (in front of the focusing lens), an irradiation pulse energy density of 0.225 J/cm^2, an effective number of laser pulses incident on any point of the sample of 500 pulses, and a sample scanning speed of 1 mm/s. This area turned out to be the opaquest. Partial damage to the TiO_2 film occurred. The second area, N2, was treated at 0.025 J/cm^2. The sample was located at 10 mm in front of the lens focus. The transparency of the film improved. For the next area of the sample (area N3), the irradiation was performed when the sample was behind the focus. This configuration adds the influence of plasma in the focal spot in air on the laser beam, but results in a diverging laser beam in the glass substrate and therefore fewer color centers in the glass substrate. An irradiation pulse energy density was 0.025 J/cm^2. The transparency of the sample improved under these treatment conditions. Further studies of the optical properties of this sample showed that the film was preserved and became more homogeneous. This experience was extended to a sample with a TiO_2 film on glass with calcination, treated with a femtosecond laser (see Fig. 4b). This sample demonstrates a sufficiently higher transparency and reveals strong hydrophilic properties.

Fig. 5 shows the optical transmission spectra of TiO_2 films on glass substrates (without calcination) before and after laser treatment using the femtosecond laser pulses at 800 nm. An interesting fact is that in the optical transmission spectra for the TiO_2 film on a glass substrate that was not annealed (N1, 0.225 J·cm^{-2}) after laser treatment, an increase in transmission is observed in both ultraviolet and red ranges. Such, at first glance, an interesting result may be associated with a violation of the integrity of the film during laser treatment and, as a result, the contribution of the transmission of the glass substrate. The transmission of area N3 of TiO_2 film (without calcination), which was treated at a lower laser power (0.025 J·cm^{-2}), has the transparency at approximately the same level within 350…1000 nm, indicating the uniformity of the film after laser treatment.

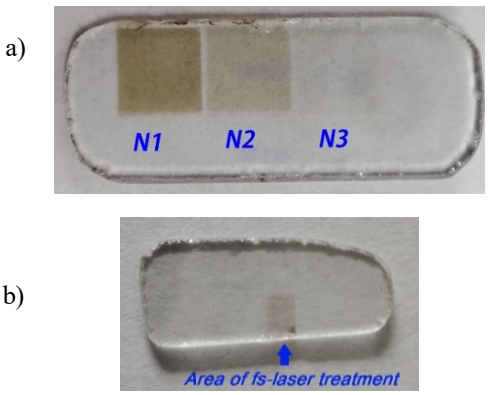

Fig. 4. (a) Image of a sample with a TiO_2 film on glass (without calcination). N1–N3 represent the areas of varying degrees of darkening caused by a femtosecond laser treatment with different irradiation energy densities, (b) image of a sample with a TiO_2 film on glass (with calcination), treated with a femtosecond laser.

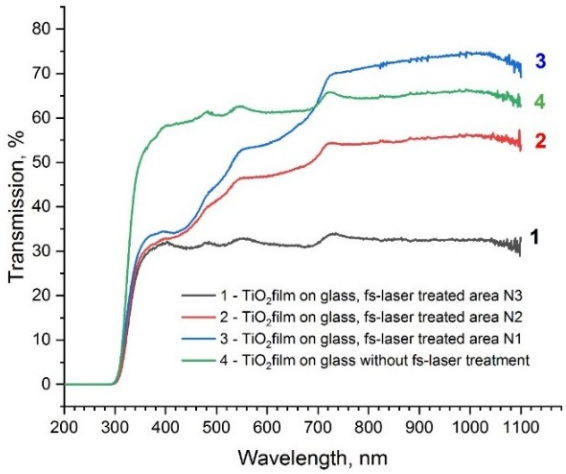

Fig. 5. Optical transmission spectra of TiO_2 films on glass substrates without calcination before and after laser treatment.

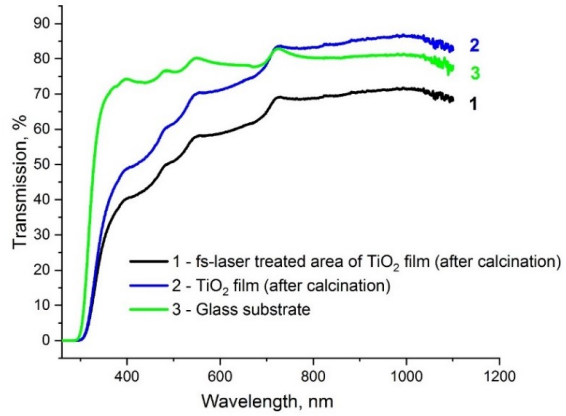

Fig. 6. Optical transmission spectra of TiO_2 film on glass substrate (with calcination) before and after femtosecond laser treatment, and optical transmission spectrum of glass substrate.

In the spectra of TiO_2 film deposited on a glass substrate and subjected to thermal treatment at 450 °C, a decrease in transmission in the entire studied region has been observed, but without change the components of the spectrum (see Fig. 6). This behaviour may indicate that during the synthesis of the films, such conditions were selected that resulted in the formation of TiO_2 films with high adhesion to the surface of the glass substrate. The film becomes homogeneous and does not undergo significant changes during the calcination and subsequent laser treatment.

Under femtosecond irradiation, a phase transformation from anatase to rutile can occur. Therefore, it is important to understand which polymorphic modification is formed under certain synthesis and post-synthetic processing parameters. During the research, it was determined that recording Raman spectra of TiO_2 films on glass substrates is methodologically difficult. It was decided to deposit the synthesized TiO_2 films on other substrates, the Raman scattering spectra of which are well known. A substrate of crystalline silicon (Si) was chosen.

Since previous studies have shown that the synthesized TiO_2 film most likely has an anatase crystal structure, we will focus on this polytype. We will also keep in mind that the phonon frequencies for the rutile structure are close in frequency to those of anatase [20–22]. Raman spectra of the two polymorphic modifications of TiO_2 (anatase and rutile) are quite distinct from each other and easily identified in pure forms, but their spectral characteristics overlap in mixtures: this makes their precise relative quantification difficult, especially when the amount of one of the two phases is small.

Anatase has a tetragonal structure and belongs to the space group $D4h19(I4/amd)$. The primitive unit cell contains two formula units of TiO_2. According to the group-theoretical analysis, the 15 phonon modes have an irreducible representation: $1A_{1g}$, + $1A_{2u}$, $+2B_{1g}$, + $1B_{2u}$ + $3E_g + 2E_u$.

The A_{1g}, B_{1g}, and E_g modes are Raman-active, while the A_{2u} and E_u modes are infrared-active. The B_{2u} mode is inactive in both the Raman and IR absorption spectra. The phonon modes at 515 and 519 cm^{-1} associated with B_{1g} and A_{1g} are usually spectrally resolved only at low temperatures. It should be noted that for the TiO_2 film on Si substrate, phonon bands characteristic of crystalline Si could be recorded (our spectrometer records only one band close to 520, 520.5 cm^{-1}). Therefore, which is the superposition of TiO_2 and Si bands.

We experimentally investigated the Raman scattering spectra for two samples (marked 2 and 3), which represented TiO_2 films deposited on Si substrates. For statistics, we measured the Raman spectra in several areas (marked area 1 and area 2) of the corresponding sample (see Fig. 7).

Analysis of Figs. 7 and 8 shows that TiO_2 films deposited on a Si substrate belong to the anatase polytype. The Raman spectra contain all main phonon modes that are characteristic of anatase polytype: strong 143 cm^{-1} ($E_g(1)$ mode), in our case very weak 197 cm^{-1} ($E_g(2)$ mode), 396 cm^{-1} (B_{1g} mode), 519 cm^{-1} (A_{1g} mode), 636 cm^{-1} ($E_g(3)$ mode). We also revealed bands associated with phonon modes of silicon (close to 301, 521, and 960 cm^{-1}).

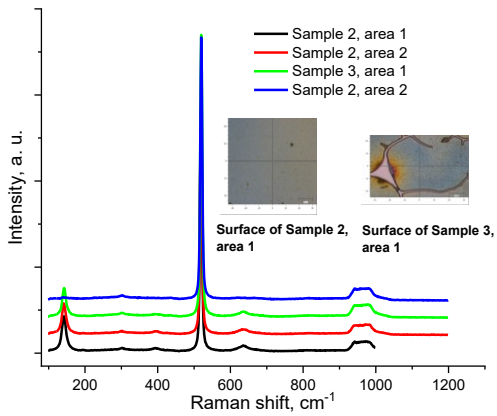

Fig. 7. Raman spectra of TiO_2 film on Si substrate: for two different samples and different areas of the corresponding sample, λ_{exc} = 532 nm, T = 300 K.

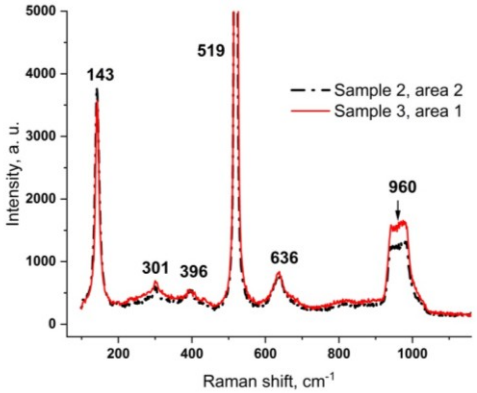

Fig. 8. Raman spectra of TiO_2 film on the surface of Si substrate: for two different samples, λ_{exc} = 532 nm, T = 300 K.

PL spectra have been studied for each regime of ultrashort laser treatment of TiO_2 films deposited on glass. PL intensity presents the recombination efficiency of photogenerated charges, which is an important factor for the photocatalytic efficiency of TiO_2 films. PL spectra of TiO_2 films (both as grown and laser treated) contain intense broad bands, namely green band close to 520 nm (2.38 eV) caused by the radiative recombination of free electrons with holes trapped around surface oxygen vacancies (V_O) and red band at 620 nm (2.0 eV) related to the defects of interstitial titanium ions (Ti^{3+}) [23–26]. These bands are components of the broad bands observed in the PL spectrum of TiO_2 films on glass substrates. The effect of the glass substrate on the PL spectra of the samples was investigated. The presence of the glass substrate causes the appearance of spectral bands close to 536 nm (2.31 eV) and 704 nm (1.76 eV). The weak PL band close to 340 nm corresponds to the exciton recombination in TiO_2. The relative intensities of these bands depend significantly on the parameters of laser treatment. The area N1 (an irradiation pulse energy density of 0.225 J·cm^{-2}, effective number of laser pulses N = 500, scanning speed 1 mm/s), which looks the darkest, demonstrates the greatest influence of the glass substrate on the PL spectrum of the TiO_2 film (see Fig. 9). Such behaviour of the PL spectra for this region is likely due to the violation of the integrity of the TiO_2 film during laser processing. At the same time, the area N3 (an irradiation pulse energy density of 0.025 J·cm^{-2}, effective number of laser pulses N = 1500, scanning speed 1 mm/s) demonstrates the greatest similarity of the PL spectrum to the PL spectrum of the untreated TiO_2 film region. Fig. 9b represents the result of subtracting the glass substrate spectrum from the PL spectrum of N3 of the laser-treated TiO_2 film on the glass substrate. PL bands close to 340 nm and 412…500 nm correspond to the free and bound excitons recombination in TiO_2 film [25]. Therefore, under selected laser parameters, the satisfactory transparency of the sample is observed, and the anatase crystal structure is preserved for the N3 area of the TiO_2 film on glass.

We expected the changes in the hydrophilic-hydrophobic balance of samples with TiO_2 on glass substrate after laser treatment. There is an interplay

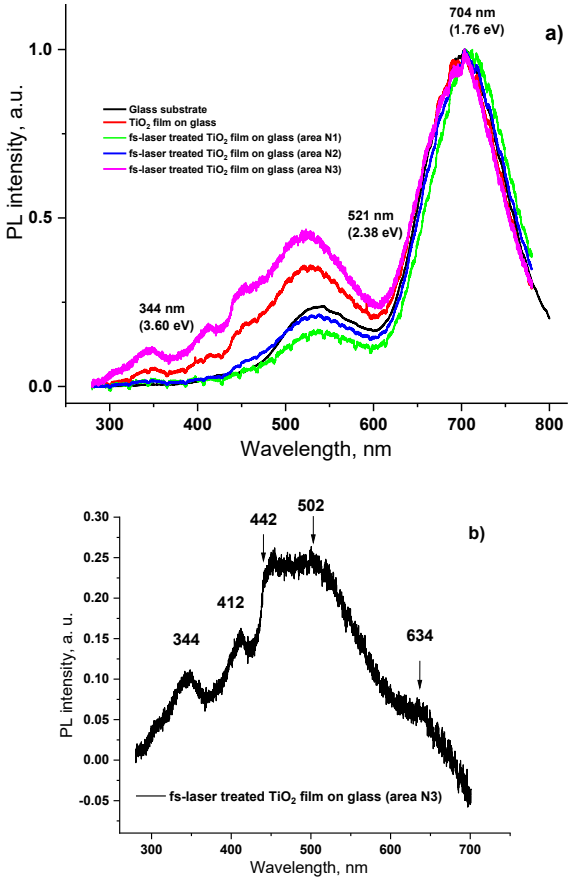

Fig. 9. PL spectra of TiO_2 films on glass substrates before and after femtosecond laser treatment, λ = 266 nm, T = 300 K (a, b). (b) represents the result of subtracting the glass substrate spectrum from the PL spectrum of area N3 of the laser-treated TiO_2 film on the glass substrate.

between different mechanisms that can contribute to these properties: improved film homogeneity after laser treatment; formation of laser-induced micro- and nano-relief; laser-induced phase transitions; products of laser-induced chemical reactions on the surface, *etc*. Our preliminary study of some samples of laser-treated TiO_2 films on glass substrates shows changes in surface wettability, namely, we observed a trend towards a decrease in contact angle of distilled water. Moreover, for some samples, the decrease in contact angle was less than 10°. These properties of laser-treated TiO_2 films on glass substrates will be studied in detail in our further research.

4. Conclusions

The developed composition of film-forming TiO_2 sols, methods of their deposition, and post-synthetic processing can be used to form coatings for various applications. The proposed approaches simplify significantly the procedure for preparing film-forming sols and reduce the time required for their preparation for application to glass substrates. The developed methods of sols deposition to glass substrates and approaches to post-synthetic processing allow obtaining homogeneous, optically transparent TiO_2 films. A femtosecond laser structuring regime was

achieved, which increased the density and uniformity of the part of the TiO_2 film on glass substrates, which remained unharmed. In particular, for the laser radiation wavelength of 800 nm, the best transparency of the TiO_2 film was achieved at an irradiation pulse energy density of 0.025 J/cm^2. The optical properties of the formed TiO_2 films on glass substrates that were studied using photoluminescence and Raman scattering spectra showed that, in our experiments, including the femtosecond laser treatment, a predominantly single anatase crystal structure is formed, and significant hydrophilic properties of the films are observed.

Acknowledgement

I.M. Dmytruk, N.I. Berezovska, P.A. Manoryk, N.I. Romanovska, G.P. Podust, Ye.S. Hrabovskyi, P.S. Khort (synthesis, post-synthetic processing, including laser treatment, morphological and spectroscopic studies) acknowledge the support from the National Research Foundation of Ukraine under the Project 2025.06/0087 "Nanostructured titanium dioxide films for coating of optical elements".

S.V. Mamykin and O.S. Kondratenko (ellipsometric analysis) express their gratitude to the Ministry of Education and Science of Ukraine for financial support within the framework of the PH/51-2024 project.

References

1. Wu P., Xue Z., Yu T., Penkov O.V. Transparent self-cleaning coatings: A review. *Coatings*. 2023. **13**. P. 1270. https://doi.org/10.3390/coatings13071270.
2. Kalinowski M., Chilmon K., Kuziak J. *et al.* Photocatalytically induced degradation of nano-TiO_2 – modified paint coatings under low-radiation conditions. *Coatings*. 2025. **15**, No 3. P. 281. https://doi.org/10.3390/coatings15030281.
3. Wei Y., Wu Q., Meng H. *et al.* Recent advances in photocatalytic self-cleaning performances of TiO_2-based building materials. *RSC Adv*. 2023. **13**. P. 20584–20597. https://doi.org/10.1039/D2RA07839B.
4. He L., Zahn D.R.T., Madeira T.I. Photocatalytic performance of sol-gel prepared TiO_2 thin films annealed at various temperatures. *Materials.* 2023. **16**. P. 5494. https://doi.org/10.3390/ma16155494.
5. Tasisa Y.E., Sarma T.K., Krishnaraj R., Sarma S. Band gap engineering of titanium dioxide (TiO_2) nanoparticles prepared via green route and its visible light driven for environmental remediation. *Res. Chem.* 2024. **11**. P. 101850. https://doi.org/10.1016/j.rechem.2024.101850.
6. Lin H., Kozuka H., Yoko T. Electrical properties of transparent doped oxide films. *J. Sol-Gel Sci. Technol*. 2000. **19**. P. 529–532. https://doi.org/10.1023/A:1008784505272.
7. Gartner M., Szekeres A., Stroescu H. *et al*. Advanced nanostructured coatings based on doped TiO_2 for various applications. *Molecules*. 2023. **28**. P. 7828. https://doi.org/10.3390/molecules28237828.
8. Bonse J., Krüger J. Structuring of thin films by ultrashort laser pulses. *Appl. Phys. A*. 2023. **129**. P. 14. https://doi.org/10.1007/s00339-022-06229-x.
9. Landis E., Phillips K., Mazur E., Friend C. Formation of nanostructured TiO_2 by femtosecond laser irradiation of titanium in O_2. *J. Appl. Phys*. 2012. **112**. Art. 063108. https://doi.org/10.1063/1.4752276.
10. Talbi A., Tchiffo Tameko C., Stolz A. *et al*. Nanostructuring of titanium oxide thin film by UV femtosecond laser beam: from one spot to large surfaces. *Appl. Surf. Sci*. 2017. **418**. P. 425–429. https://doi.org/10.1016/j.apsusc.2017.02.033.
11. Talbi A., Semmar N., Tabbal M. *et al.* Femtosecond laser irradiation of titanium oxide thin films: accumulation effect under IR beam. *Appl. Phys. A.* 2020. **126**. P. 390. https://doi.org/10.1007/s00339-020-03568-5.
12. Segovia P., Wong A., Santillan R. *et al*. Multi-phase titanium oxide LIPSS formation under fs laser irradiation on titanium thin films in ambient air. *Opt. Mater. Express*. 2021. **11**, No 9. P. 2892–2906. https://doi.org/10.1364/OME.431210.
13. Medvids A., Onufrijevs P., Kaupužs J. *et al.* Anatase or rutile TiO_2 nanolayer formation on Ti substrates by laser radiation: Mechanical, photocatalytic and antibacterial properties. *Opt. Laser Technol*. 2021. **138**. P. 106898. https://doi.org/10.1016/j.optlastec.2020.106898.
14. Bugaychuk S., Iljin A., Telbiz G. *et al.* Nonlinear all-optical light valves fabricated on mesoscopic Ti-, Si-substrates. *J. Mol. Liq*. 2018. **267**. P. 34–37. https://doi.org/10.1016/j.molliq.2018.01.170.
15. Jellison G.E., Jr, Modine F.A. Parameterization of the optical functions of amorphous materials in the interband region. *Appl. Phys. Lett*. 1996. **69**, No 3. P. 371–373. https://doi.org/10.1063/1.118064.
16. Golovynskyi S., Ievtushenko A., Mamykin S. *et al.* High transparent and conductive undoped ZnO thin films deposited by reactive ion-beam sputtering. *Vacuum*. 2018. **153**. P. 204–210. https://doi.org/10.1016/j.vacuum.2018.04.019.
17. Kryshtab T., Borkovska L., Cortés Herrera R.B. *et al.* Influence of terbium doping and annealing on the structural and optical characteristics of sputtered zinc oxide thin films. *Crystals*. 2023. ***13***. P.1200. https://doi.org/10.3390/cryst13081200.
18. Vasin A.V., Gomeniuk Y.V., Lytvyn P.M. *et al.* Structural insight into nanoscale inhomogeneity of electrical properties in highly conductive polycrystalline ZnO thin films doped using methane. *J. Phys. D: Appl. Phys*. 2024. **57**. P. 155101. https://doi.org/10.1088/1361-6463/ad1791.
19. Mero M., Liu J., Sabbah A.J. *et al*. Scaling laws of femtosecond laser pulse induced breakdown in oxide films. *Phys. Rev. B*. 2005. **71**. Art. 115109. https://doi.org/10.1103/PhysRevB.71.115109.
20. Porto S., Fleury P., Damen T. Raman spectra of TiO_2, MgF_2, ZnF_2, FeF_2, and MnF_2. *Phys. Rev*. 1967. **154**. P. 522–526. https://doi.org/10.1103/PhysRev.154.522.
21. Ohsaka T., Izumi F., Fujiki Y. Raman spectrum of anatase, TiO_2. *J. Raman Spectrosc*. 1978. **7**, No 6. P. 321–324. https://doi.org/10.1002/jrs.1250070606.
22. Ocana M., Garcia-Ramos J.V., Serna C.J. Low-temperature nucleation of rutile observed by Raman spectroscopy during crystallization of TiO_2. *J. Am. Ceram.*

Soc. 1992. **75**, No 7. P. 2010–2012. https://doi.org/10.1111/j.1151-2916.1992.tb07237.x.
23. Jin C., Liu B., Lei Z. *et al.* Structure and photoluminescence of the TiO_2 films grown by atomic layer deposition using tetrakis-dimethylamino titanium and ozone. *Nanoscale Res. Lett.* 2015. **10**. Art. 95. https://doi.org/10.1186/s11671-015-0790-x.
24. Abazovic N.D., Comor M.I., Dramicanin M.D. *et al.* Photoluminescence of anatase and rutile TiO_2 particles. *J. Phys. Chem. B*. 2006. **110**, No 50. P. 25366–25370. https://doi.org/10.1021/jp064454f.
25. Pallotti D.K., Passoni L., Maddalena P. *et al.* Photoluminescence mechanisms in anatase and rutile TiO_2. *J. Phys. Chem. C*. 2017. **121**, No 16. P. 9011–9021. https://doi.org/10.1021/acs.jpcc.7b00321.
26. Sittishoktram M., Soontaranon S., Jevasuwan W. *et al.* Influence of point defects on phase transformation and optical properties of TiO_2 thin films *via* multilayering deposition technique. *Mater. Chem. Phys.* 2021. **272**. Art. 124859. https://doi.org/10.1016/j.matchemphys.2021.124859.

Authors and CV

Igor M. Dmytruk, Doctor of Sciences in Physics and Mathematics, Professor, Head of Experimental Physics Department, Physics Faculty at the Taras Shevchenko National University of Kyiv. Author of over 150 publications. The area of his scientific interests includes laser spectroscopy of highly excited semiconductors: studies of the excitonic processes in solid state, nanoparticles, clusters; ultrafast spectroscopy of different materials; computer calculations and simulations.
E-mail: igor_dmytruk@knu.ua,
http://orcid.org/0000-0001-9482-8746

Nataliya I. Berezovska, PhD in Physics and Mathematics (Optics, Laser Physics, 2005), Senior researcher at the Physics Faculty of the Taras Shevchenko National University of Kyiv. Author of about 60 publications. The area of her scientific interests includes the study of excitonic processes in solid state, plasmonic photovoltaics, laser-induced transformations in metals, semiconductors, and hybrid metal/semiconductor systems. https://orcid.org/0000-0002-6967-6426

Pavlo S. Khort, PhD student at the Physics Faculty of the Taras Shevchenko National University of Kyiv. Author of 10 peer-reviewed papers. The area of his scientific interests includes optical properties of hybrid molecular plasmonics nanosystems. https://orcid.org/0000-0002-1169-2431, e-mail: pavlokhort@gmail.com

Petro A. Manoryk, Doctor of Sciences in Chemistry, Head of Department at the L.V. Pisarzhevskii Institute of Physical Chemistry, NAS of Ukraine. He has authored over 80 publications, 40 patents, and 2 text-books. The area of his scientific interests includes coordination chemistry of bimetals, sol-gel synthesis of metaloxides compounds.
E-mail: manorik01@gmail.com,
https://orcid.org/ 0000-0001-7197-0707

Nataliia I. Romanovska, PhD in Chemistry (Physical Chemistry, 2021), Researcher at the L.V. Pisarzhevskii Institute of Physical Chemistry, NAS of Ukraine. She has authored over 16 publications and 15 patents. The area of her scientific interests includes sol-gel synthesis of different functional materials.
E-mail: nat.romanovska@gmail.com,
https://orcid.org/0000-0002-3996-6107

Galyna P. Podust, PhD in Physics and Mathematics (Solid State Physics), Senior researcher at the Taras Shevchenko National University of Kyiv. Author of over 80 scientific publications. The area of her scientific interests includes photonics, spectroscopy, and semiconductor physics.
E-mail: podust@univ.kiev.ua,
https://orcid.org/0000-0002-2528-1895

Yevhen S. Hrabovskyi, Engineer 1 class at the Taras Shevchenko National University of Kyiv. He received a Master's degree at the Taras Shevchenko National University of Kyiv in 2012. Author of 6 peer-reviewed papers. The area of his scientific interests includes laser-induced transformations in metals, semiconductors, hybrid metal/semiconductor systems, and plasmonic photovoltaics.
E-mail: hrabovskyi@knu.ua
https://orcid.org/0000-0003-4078-0569

Olga S. Kondratenko, PhD in Physics and Mathematics, Senior researcher at the Department of Diagnostics of semiconductor materials, structures and devices, Laboratory of spectral ellipsometry, V. Lashkaryov Institute of Semiconductor Physics, NAS of Ukraine. The area of scientific interests includes optoelectronics, plasmonics, optics, nanophotonics, thin films. E-mail: kondratenko@isp.kiev.ua,
https://orcid.org/0000-0003-1948-4431

Volodymyr R. Romanyuk, PhD, Senior researcher at the Department of Kinetic Phenomena and Polaritonics, V. Lashkaryov Institute of Semiconductor Physics, NASU. Authored more than 50 articles. The area of scientific interests includes optical materials science, optical diagnostics based on visible and infrared spectroscopy methods, and ellipsometry. E-mail: romanyuk@isp.kiev.ua, https://orcid.org/0000-0002-0068-5973

Sergii V. Mamykin, PhD, Head of the Department of Kinetic Phenomena and Polaritonics at the V. Lashkaryov Institute of Semiconductor Physics, NAS of Ukraine. Author of over 90 publications and 5 patents. The area of his scientific interests includes plasmonics, sensorics and physics of photodetectors. E-mail: mamykin@isp.kiev.ua, http://orcid.org/0000-0002-9427-324X

Authors' contributions

Dmytruk I.M.: conceptualization, supervision, formal analysis, writing – original draft, methodology, and realization of femtosecond laser treatment.
Berezovska N.I.: conceptualization, photoluminescence measurements, writing – original draft.
Manoryk P.A.: key ideas of discovering the composition of the reaction mixture, conceptualization, writing – review & editing.
Romanovska N.I.: sample preparation, post-synthesis treatment, writing – original draft.
Podust G.P.: Raman spectra measurements, manuscript preparation.
Hrabovskyi Ye.S.: femtosecond laser processing of samples.
Khort P.S.: SEM measurements, visualization.
Kondratenko O.S.: formal analysis, ellipsometric parameters investigation.
Romanyuk V.R.: determining the samples parameters, writing – review and editing.
Mamykin S.V.: conceptualization, methodology, ellipsometric analysis, writing – review & editing.

Фемтосекундна лазерна обробка плівок діоксиду титану, отриманих золь-гель методом

І.М. Дмитрук, Н.І. Березовська, П.А. Манорик, Н.І. Романовська, Г.П. Подуст, Є.С. Грабовський, П.С. Хорт, О.С. Кондратенко, В.Р. Романюк, С.В. Мамикін

Анотація. Здатність плівок TiO_2 до самоочищення та фотокаталізу має вирішальне значення для покриттів оптичних елементів, коли вони працюють у складних навколишніх умовах. У процесі нашого дослідження вибрано оптимальний хімічний склад реакційної золь-гель суміші та умови для формування плівок TiO_2 методом spin-coating. Еліпсометричні дослідження показали, що перед кальцинуванням при 450 °C осаджена плівка TiO_2 на склі мала товщину 247 нм та була достатньо пористою із суттєвою шорсткістю. Після кальцинування товщина плівки TiO_2 зменшилась до 89 нм, а також плівка стала значно щільнішою. Подальшу модифікацію плівок TiO_2 було проведено за допомогою фемтосекундних лазерних імпульсів з довжиною хвилі 800 нм. Фемтосекундна лазерна обробка плівок TiO_2 привела до утворення лазерно-індукованих поверхневих елементів, зокрема наночастинок та нанотріщин. Вибрані умови фемтосекундної лазерної обробки мали на меті зберегти достатню прозорість плівки TiO_2, що було досягнуто при густині енергії імпульсу опромінення 0,025 Дж/см². Оброблена лазером поверхня демонструє покращені гідрофільні властивості. Оптичні властивості плівок TiO_2 на скляних підкладках, досліджені за допомогою фотолюмінесценції та раманівського розсіювання, показали, що післясинтетична обробка, включаючи фемтосекундну лазерну обробку, приводить до формування переважаючої кристалічної фази анатазу.

Ключові слова: діоксид титану, тонка плівка, золь-гель метод, фемтосекундні лазерні імпульси, лазерно-індуковані поверхневі структури, фотолюмінесценція, раманівське розсіювання.